Observation of transverse interference fringes on an atom laser beam

R. G. Dall, L. J. Byron and A. G. Truscott

ARC Centre of Excellence for Quantum-Atom Optics.
Research School of Physical Sciences and Engineering, Australian National University, Canberra, ACT 0200, Australia.

G. R. Dennis, M. T. Johnsson, M. Jeppesen and J. J. Hope

ARC Centre of Excellence for Quantum-Atom Optics.
Department of Physics, Australian National University, Canberra, ACT 0200, Australia.

andrew.truscott@anu.edu.au

http://www.rsphysse.anu.edu.au/hebec/

Abstract: Using the unique detection properties offered by metastable helium atoms we have produced high resolution images of the transverse spatial profiles of an atom laser beam. We observe fringes on the beam, resulting from quantum mechanical interference between atoms that start from rest at different transverse locations within the outcoupling surface and end up at a later time with different velocities at the same transverse position. Numerical simulations in the low output-coupling limit give good quantitative agreement with our experimental data.

OCIS codes: (020.0020) Atomic and Molecular Physics; (020.1475) Bose-Einstein Condensates

References and links

1. M.-O. Mewes, M. R. Andrews, D. M. Kurn, D. S. Durfee, C. G. Townsend, and W. Ketterle, "Output coupler for Bose-Einstein condensed atoms," Phys. Rev. Lett. **78**, 582-585 (1997).
2. P. Bouyer and M. A. Kasevich, "Heisenberg-limited spectroscopy with degenerate Bose-Einstein gases," Phys. Rev. A **56**, R1083-R1086 (1997).
3. Ying-Ju Wang, Dana Z. Anderson, Victor M. Bright, Eric A. Cornell, Quentin Diot, Tetsuo Kishimoto, Mara Prentiss, R. A. Saravanan, Stephen R. Segal, and S. Wu, "Atom Michelson Interferometer on a chip using a Bose-Einstein condensate," Phys. Rev. Lett. **94**, 090405 (2005).
4. Y. Shin, C. Sanner, G.-B. Jo, T. A. Pasquini, M. Saba, W. Ketterle, and D. E. Pritchard,"Interference of Bose-Einstein condensates split with an atom chip," Phys. Rev. A **72**, 021604(R) (2005).
5. J.-F. Riou, W. Guerin, Y. Le Coq, M. Fauquembergue, V. Josse, P. Bouyer, and A. Aspect, "Beam quality of a Nonideal atom laser," Phys. Rev. Lett. **96**, 070404 (2006).
6. Th. Busch, M. Kohl, T. Esslinger, and K. Mølmer, "Transverse mode of an atom laser," Phys. Rev. A **65**, 043615 (2002).
7. T. Kramer, C. Bracher, and M. Kleber, "Matter waves from quantum sources in a force field," J. Phys. A **35**, 8361-8372 (2002).
8. M. Kohl, Th. Busch, K. Molmer, T. W. Hansch, and T. Esslinger, "Observing the profile of an atom laser beam," Phys. Rev. A **72**, 063618 (2005).
9. A. Robert, O. Sirjean, A. Browaeys, J. Poupard, S. Nowak, D. Boiron, C. I. Westbrook, and A. Aspect, "A Bose-Einstein condensate of metastable atoms," Science **292**, 461-464, (2001).
10. F. Pereira Dos Santos, J. Léonard, Junmin Wang, C. J. Barrelet, F. Perales, E. Rasel, C. S. Unnikrishnan, M. Leduc, and C. Cohen-Tannoudji, "Bose-Einstein Condensation of Metastable Helium," Phys. Rev. Lett. **86**, 3459-3462 (2001).

#87989 - $15.00 USD Received 3 Oct 2007; revised 28 Nov 2007; accepted 7 Dec 2007; published 12 Dec 2007

11. A. S. Tychkov, T. Jeltes, J. M. McNamara, P. J. J. Tol, N. Herschbach, W. Hogervorst, W. Vassen, "Metastable helium Bose-Einstein condensate with a large number of atoms," Phys. Rev. A **73**, 031603(R) (2006).
12. K.G.H. Baldwin, "Metastable helium: Atom optics with nano-grenades," Cont. Phys. **46**, 105-120 (2005).
13. S. Moal, M. Portier, J. Kim, J. Dugue, U. D. Rapol, M. Leduc, and C. Cohen-Tannoudji, "Accurate determination of the scattering length of metastable helium atoms using dark resonances between atoms and exotic molecules," Phys. Rev. Lett. **96**, 023203 (2006).
14. C. Blondel, C. Delsart, and F. Dulieu, "The Photodetachment Microscope," Phys. Rev. Lett. **77**, 3755-3758 (1996).
15. I. Bloch, T. W. Hansch, and T. Esslinger, "Atom laser with a cw output coupler," Phys. Rev. Lett. **82**, 3008-3011 (1999).
16. XMDS documentation and source code available from http://www.xmds.org
17. Ch. J. Borde, "Theoretical tools for atom optics and interferometry," C. R. Acad. Sci. Paris, t. 2, Serie IV, 509-530 (2001).
18. R. G. Dall, and A. G. Truscott, "Bose-Einstein condensation of metastable helium in a biplanar quadrupole Ioffe configuration trap," Opt. Commun. **270**, 255-261 (2007).
19. J. A. Swansson, R. G. Dall and A. G. Truscott, "An intense cold beam of metastable helium," Appl. Phys. B **86**, 485-489 (2007).
20. C. J. Dedman, R. G. Dall, L. J. Byron and A. G. Truscott, "Active cancellation of stray magnetic fields in a Bose-Einstein condensation experiment," Rev. Sci. Instrum. **78**, 024703 (2007).
21. I. Bloch, T. W. Hansch, and T. Esslinger, "Measurement of the spatial coherence of a trapped Bose gas at the phase transition," Nature **403**, 166-170 (2000).
22. A. Òttl, S. Ritter, M. Kohl, and T. Esslinger, "Correlations and counting statistics of an atom laser," Phys. Rev. Lett. **95**, 090404 (2005).
23. N. P. Robins, A. K. Morrison, J. J. Hope and J. D. Close, "Limits to the flux of a continuous atom laser," Phys. Rev. A **72**, 031606(R) (2005).
24. M. Jeppesen, J. Dugué, G. Dennis, M. T. Johnsson, C. Figl, N. P. Robins, J. D. Close, "Approaching the Heisenberg limit in an atom laser," e-print arXiv:quant-ph/07040291.

1. Introduction

Atoms coherently output-coupled from a Bose-Einstein condensate (BEC) form a coherent beam of matter waves, or 'Atom laser' [1]. Like its optical counterpart, the atom laser has the potential to revolutionise future atom interferometric sensors [2, 3, 4], in which a high flux of collimated atoms is required. The ultimate performance of such sensors will rely on the signal-to-noise ratio with which atoms in the atom laser beam can be detected. In the case of a metastable helium atom laser, its constituent atoms are not in their true electronic ground state, but rather in an excited state containing 20 eV of energy. This large internal energy is enough to liberate electrons from a surface when struck by the atom, making detection of single metastable atoms possible. It is this single atom detection property that makes a metastable atom laser not only a promising candidate for future atom laser applications but also as a high resolution probe of fundamental atom laser properties.

Unlike an optical laser, the particles in an atom laser interact with each other by scattering. At ultracold temperatures this scattering can be characterised by a single parameter, the s-wave scattering length. In most cases these interactions are small since the average density in a typical continuous wave (cw) atom laser beam is low. However, as the atoms in the beam are coupled out, they probe the high density of the BEC via the same interactions, and experience a large repulsive force (so-called 'mean field' repulsion). These interactions heavily distort the atom laser beam, resulting in a profile that exhibits a double peaked structure due to classical effects, referred to as 'caustics' [5].

Besides these large-scale classical effects, it has been predicted that interference fringes should be present on an atom laser beam. Atoms starting from rest at different transverse locations within the outcoupling surface can end up at a later time with different velocities at the same transverse position, leading to quantum mechanical interference [6, 7].

A few previous experimental studies of atom laser profiles, all using rubidium atom lasers, have been carried out. Riou *et al.* [5] observed the appearance of caustics in their atom laser

#87989 - $15.00 USD Received 3 Oct 2007; revised 28 Nov 2007; accepted 7 Dec 2007; published 12 Dec 2007

beam profile, as predicted theoretically by Busch *et al.* [6]. Kohl *et al.* [8] used a curved mirror to 'magnify' the transverse density distribution of their atom laser beam to produce high resolution absorption images. In this paper we make use of the unique detection capabilities offered by metastable atoms [9, 10, 11, 12] to image the two-dimensional transverse profile of our radio-frequency (RF) output-coupled atom laser beam. Moreover, we observe for the first time interference fringes on an atom laser beam, demonstrating the transverse coherence of an atom laser.

Compared to previously produced rubidium atom lasers, our condensate is large compared to the gravitational sag of the magnetic trap. This is due to the relatively large s-wave scattering length [13] and low mass for ^{4}He* in combination with the tight confinement that is possible. For such a system, RF output coupling leads to output-coupling surfaces that are oblate spheres rather than planes, as is the case of previously studied atom lasers [15]. This output-coupling geometry leads to a 'fountaining' effect (see Fig. 1), in which atoms output coupled above the trap centre experience an upward force. Since the output-coupling surface is almost symmetric around the centre of the magnetic trap, the result is that initially the output-coupled atom cloud contains atoms traveling up and down. This creates unusual dynamics, in which some atoms 'fountain' up and then drop back through the condensate. The resulting transverse atom laser profiles exhibit a shadowed region, cast by the condensate, since atoms attempting to pass back through the condensate are pushed off axis due to the dominant mean field repulsion.

2. Theory

Rubidium atom laser beam profiles are typically modelled [5] using a two-step process where the wavefunction is first found on the edge of the condensate using the WKB approximation, and then propagated through free space using a Kirchoff-Fresnel diffraction integral over the surface of the condensate. In both of these steps, the nonlinear beam-beam interactions are neglected. In He* experiments, the nonlinear interaction strength U is 28 times larger than for Rubidium (due to the larger scattering length and the smaller atomic mass), so the nonlinear beam-beam interactions cannot be neglected inside the condensate, although sufficiently far below the condensate, the atom laser beam density will have reduced sufficiently for it to be negligible. From this point down, the nonlinear beam-beam interactions can be neglected and a Kirchoff-Fresnel diffraction integral used.

To model our experiment we use a two-step method where we first solve the 3D Gross-Pitaevskii (GP) equation for the atom laser beam wave function in the volume between the classical turning point of the atom laser beam above the condensate down to a point far enough below the condensate such that the nonlinear beam-beam interaction becomes negligible. This wavefunction is then used to solve for the atom laser beam density on the detector by performing a Kirchoff-Fresnel diffraction integral over a plane below the condensate. The Gross-Pitaevskii equations describing an outcoupled atom laser are

$$i\hbar\frac{\partial\Psi_t}{\partial t} = -\frac{\hbar^2\nabla^2}{2m}\Psi_t + V_{\text{trap}}(\mathbf{x})\Psi_t - mgz\Psi_t + U(|\Psi_t|^2 + |\Psi_u|^2)\Psi_t + \hbar\Omega\Psi_u, \tag{1}$$

$$i\hbar\frac{\partial\Psi_u}{\partial t} = -\frac{\hbar^2\nabla^2}{2m}\Psi_u - mgz\Psi_u + U(|\Psi_t|^2 + |\Psi_u|^2)\Psi_u + \hbar\Omega\Psi_t, \tag{2}$$

where Ψ_t and Ψ_u are the trapped and untrapped fields respectively, $V_{\text{trap}}(\mathbf{x}) = \frac{1}{2}m(\omega_x^2x^2 + \omega_y^2y^2 + \omega_z^2z^2)$ is the trapping potential, ω_x, ω_y, and ω_z are the trapping frequencies, U is the nonlinear interaction strength, and Ω is the Rabi frequency of the RF outcoupling. In this work, we have assumed that the outcoupling rate is sufficiently low such that the beam's back-action on the condensate can be neglected, allowing us to set the terms involving Ψ_u Eq. 1 to zero

#87989 - $15.00 USD Received 3 Oct 2007; revised 28 Nov 2007; accepted 7 Dec 2007; published 12 Dec 2007

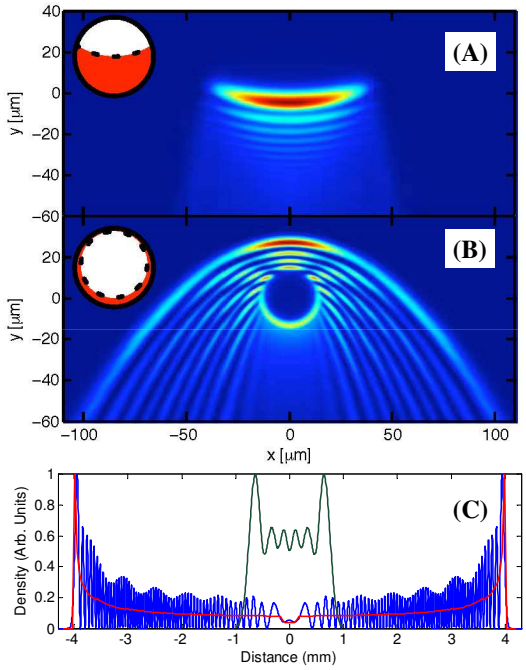

Fig. 1. Near field simulations of atom laser profiles, showing vastly different output dynamics depending whether output-coupling takes place on (A) planes or on (B) oblate spheres. The output-coupling regions (dashed line), relative to the BEC (circle), used to create these plots are shown diagrammatically in the upper left corner of each plot. In both cases the BEC is located at the origin, with radial trapping frequencies of 50 Hz and 460 Hz for (A) and (B) respectively. The resulting far field atom laser profiles as calculated at our detector for (A) and (B) are shown in (C). The green profile results from the near field distribution shown in (A). The blue and red profiles result from the near field distribution shown in (B) and are calculated using the Gross-Pitaevskii equation and classical mechanics respectively. The classical simulation treats the atoms as classical particles that begin on the outcoupling surface and are pushed from the BEC due to a potential that is given by the mean field repulsion; the resulting two-lobe caustic structure is clearly visible.

in our simulations. Consequently any effects such as local condensate depletion and excitation of higher-order condensate modes are ignored in our model. These equations were integrated numerically with an adaptive fourth-fifth order Runge-Kutta algorithm using the open source package XMDS [16].

Once the steady state for the atom laser beam has been found from the GP equations, the wavefunction at the detector is found by using a Kirchoff-Fresnel diffraction integral over an infinite plane below the condensate,

$$\Psi(\mathbf{r}) = \int_S d\mathbf{S}' \cdot \left[G_E(\mathbf{r},\mathbf{r}')\nabla'\Psi(\mathbf{r}') - \Psi(\mathbf{r}')\nabla' G_E(\mathbf{r},\mathbf{r}') \right], \tag{3}$$

where $G_E(\mathbf{r},\mathbf{r}')$ is the time-independent Green's function for energy E, and potential $V = -mgz$ [17]. Although the integral in Eq. 3 is a surface integral, for simplicity we follow [5] and neglect divergence in the weak trapping direction and only consider lines along the plane of the strong trapping axes, making the integral one dimensional.

The complicated dynamics of an atom laser with an output-coupling surface that is an oblate

#87989 - $15.00 USD Received 3 Oct 2007; revised 28 Nov 2007; accepted 7 Dec 2007; published 12 Dec 2007

sphere is predicted by our model to produce atom laser profiles with two sets of interference fringes. The first set of fringes are due to interference between atoms that initially go upwards and those that go downwards. These are high spatial frequency fringes since the transverse velocity difference of these atoms is relatively large. Interestingly, analogous interference effects have been observed in photodetachment experiments [14]. This fringe pattern is modulated by a second set of fringes with a smaller spatial frequency that are due to interference between atoms starting with slightly different transverse positions. This contrast in dynamics is shown in Fig. 1(c) where the results of a numerical simulation of a He* atom laser beam profile generated from condensates with different radial trapping frequencies is plotted.

3. Experiment and Results

To study the atom laser profile, we use atoms RF output-coupled from a He* BEC. Our experimental setup for creating a He* BEC has been reported elsewhere [18]. Briefly, we use a cryogenic beamline to produce a He* MOT. Atoms are extracted from this low vacuum magneto-optic trap (MOT) into a high vacuum MOT via an LVIS$^+$ setup [19]. Atoms are transfered from the MOT into a BiQUIC magnetic trap, where a BEC is produced using forced RF evaporative cooling. Using this setup we are able to create almost pure BECs containing up to 5×10^6 atoms. Our experimental apparatus allows us to smoothly change the radial trapping frequencies from 100 Hz to 1020 Hz, while the axial frequency is a constant 55 Hz. To ensure the stability of our atom laser a number of experimental techniques are employed. Firstly, we stabilise the currents through our magnetic trap coils to 1 part in 10^5, which amounts to less than 10 μG of magnetic field noise. Secondly, active compensation of stray background magnetic fields [20] is used to reduce the amplitude of stray AC fields to below 20 μG and long term DC drifts to 10 μG. Finally, to minimise shot-to-shot variations, temperature controlled water is used to thermally control the magnetic trap.

Coherence is an important property of any laser. For an atom laser both first [21] and second order coherence [22] in the longitudinal direction have been demonstrated. Transverse coherence of weakly outcoupled atom laser beams has not, due to the difficulty of resolving the small scale fringe structure and the magnetic trap stability required. Our experiments are analogous to diffraction of light through a single slit, where interference results from waves emanating from an extended source taking different paths to the same point on a screen. When looking at a cross section of a beam of light, the length over which the phase is correlated is called the transverse coherence length. To demonstrate the transverse coherence of our atom laser beam we image the atom laser beam profile 4 cm below the BEC using a double stacked multi-channel plate (MCP) in combination with a phosphor screen. We image the phosphor screen with a CCD camera, resulting in an imaging resolution of approximately 150 μm. Although this resolution is too low to observe the fast fringes predicted by our simulations, it is more than adequate to detect the slower fringes. To remove any uniformities caused by spatial variations in the gain of our MCP, we devide all our images by a flat field image, produced by dropping atoms from a MOT onto our detector. Since the MOT temperature is of order $\sim$ 1 mK, the spatial profile of the MOT uniformly illuminates our MCP.

For these measurements we use a trap with radial frequency $f_r = 1020$ Hz, tune our output-coupling frequency to the centre of the BEC, and produce cw atom lasers with a duration of 20 ms. Fig. 2 (upper plot) shows the full two-dimensional raw atom laser profile on our MCP when a Rabi frequency of 500 Hz is used. The image is taken over the full duration of the atom laser, and thus is integrated over time. Also shown is the theoretical line profile (lower trace) which is in good agreement with experiment (middle trace). Note that the symmetry of the atom laser beam allows us to average our experimental profile by reflection through the origin. This tends to average out any structure that does not occur on both sides of the atom laser beam.

#87989 - $15.00 USD Received 3 Oct 2007; revised 28 Nov 2007; accepted 7 Dec 2007; published 12 Dec 2007

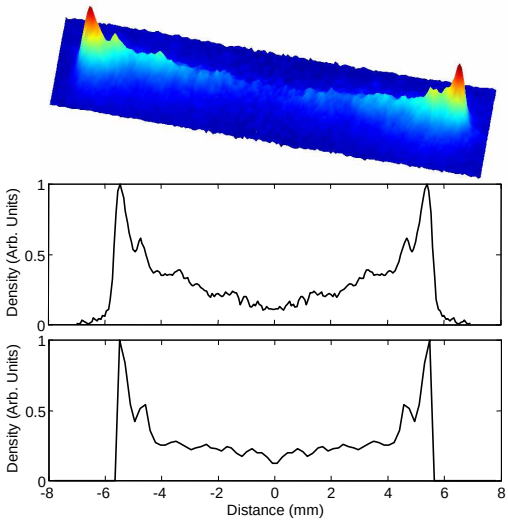

Fig. 2. Comparison of theory and experiment. Upper trace shows an experimental 2-D MCP image of the transverse profile of an atom laser (image size is 13 mm by 3.4 mm). Middle trace is an averaged profile taken through the centre of the 2-D image. Lower trace is the expected theoretical profile corresponding to the experimental conditions.

We have also averaged the theoretical profile, using the resolution of our detection system. At this relatively low output-coupling power, we observe only one interference maximum, located at ± 4.6 mm. We also observe a dark area in the central region, caused by the BEC casting a shadow in the atom laser beam.

While most of the salient features are predicted well by the theoretical model (i.e. width, position of the interference fringes, and observed shadow) there is some disagreement in the general shape probably due to back-action [23] of the atom laser on the BEC. These differences become more obvious at higher output-coupling powers, where back-action effects are more pronounced. As a single simulation of the experiment takes 2000 hours of CPU time on a supercomputer, it is currently not feasible to include back-action effects as this would significantly increase the simulation time required. Despite this limitation, our model predicts higher visibility interference fringes for higher Rabi frequencies, which is a trend observed in the experiment. Fig. 3 shows the appearance of high contrast interference fringes on our atom laser profile when a output coupling Rabi frequency of 1 kHz is used.

Let us now turn our attention to the beam quality of an atom laser beam, in the context of its application to future technologies. It is clear that the complicated mode structures exhibited by our He* atom laser are far from ideal when one considers possible applications. However, the atom laser profiles previously shown are at the extreme of non-ideal, since we have output-coupled from the centre of the condensate and used relatively tight radial trapping frequencies. In principle, both these effects can be minimised by reducing the trapping frequency and by output-coupling from the very edge of the condensate where the density is lower and where the effects of mean field repulsion will be less [8]. Fig. 4 shows a series of 2-D atom laser profiles with axial and radial magnetic trap frequencies of (A)$f_a = 55$ Hz, $f_r = 460$ Hz and (B)$f_a = 55$ Hz, $f_r = 113$ Hz in which we have varied the position of the output-coupling surface inside the BEC. The resulting profiles display the same basic shape, converging to almost a gaussian as the output-coupling surface is tuned to the very edge of the condensate. This series

#87989 - $15.00 USD Received 3 Oct 2007; revised 28 Nov 2007; accepted 7 Dec 2007; published 12 Dec 2007

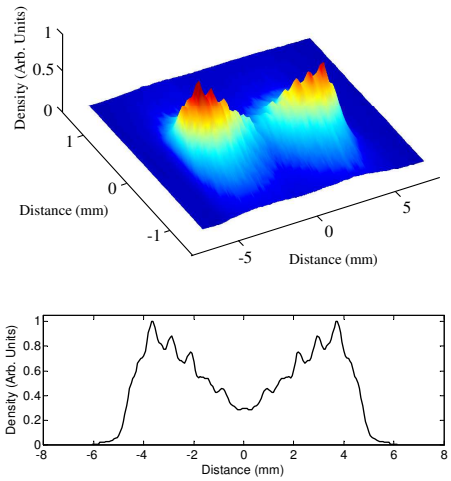

Fig. 3. Experimental MCP image (upper plot) and cross-section (lower plot) showing interference fringes. Upper trace is the raw 2-D image, while the lower trace is an averaged profile.

of measurements demonstrates that it is possible to obtain a less structured mode profile for a He* atom laser, although operating at such low trapping frequencies and operating near the edge of the condensate is not ideal since this is where we have the highest degree of technical noise. A better alternative is to output-couple using optical Raman transitions, which have been shown to produce atom laser beams with higher mode quality for rubidium atom lasers [24].

4. Conclusion

In summary, we have taken high resolution 2-D images of a He* atom laser beam profile. For low output-coupling powers, we see good agreement between the experimental data and theoretical simulations of our system. In particular, the interference fringes predicted by the theory are observed. For higher output-coupling powers, we see multiple high contrast fringes, demonstrating the transverse coherence of our atom laser beam. The dynamics of our atom laser is markedly different to others previously studied, and give rise to quite unique beam profiles which are far from gaussian. We demonstrate, however, that by reducing the radial trap frequency and output-coupling from the edge of the condensate that the beam profile can be significantly improved, and may yet be useful for future atom optic devices.

Acknowledgments

The authors wish to acknowledge the technical assistance of Stephen Battisson in the design and construction of the He* beamline, Colin Dedman for producing the magnetic trap switching circuitry and Ken Baldwin for careful reading of the manuscript. This work is supported by the Australian Research Council Centre of Excellence for Quantum-Atom Optics and the APAC National Supercomputing Facility.

#87989 - $15.00 USD Received 3 Oct 2007; revised 28 Nov 2007; accepted 7 Dec 2007; published 12 Dec 2007

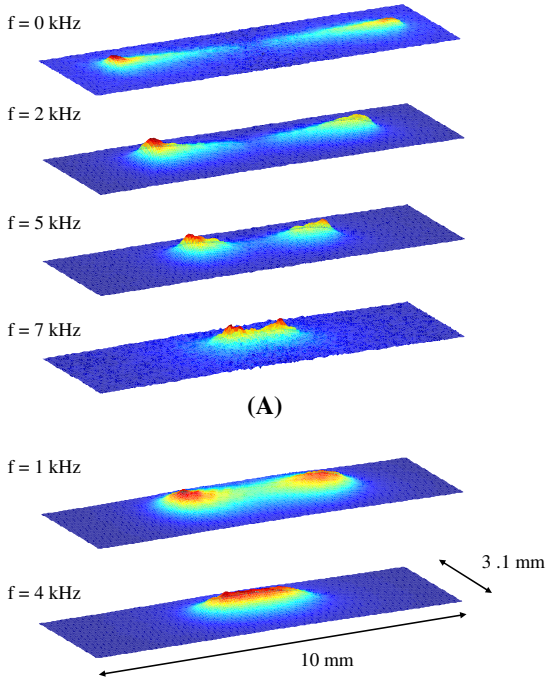

Fig. 4. Experimental two-dimensional images of a He* atom laser beam. Successive images are plotted in which the detuning of the RF, shown to the left of each image, is moved from the central high density region of the condensate to the edge of the condensate. For comparison two configurations are shown for which the radial trapping frequency is significantly different (A) $f_a = 55$ Hz, $f_r = 460$ Hz and (B) $f_a = 55$ Hz, $f_r = 113$ Hz.

#87989 - $15.00 USD Received 3 Oct 2007; revised 28 Nov 2007; accepted 7 Dec 2007; published 12 Dec 2007